Inorg. Chem. **2003**, *42*, 7326–7338

Organometallic Chemistry of Azuliporphyrins: Synthesis, Spectroscopy, Electrochemistry, and Structural Characterization of Nickel(II), Palladium(II), and Platinum(II) Complexes of Azuliporphyrins†

Timothy D. Lash,* Denise A. Colby, Shelley R. Graham, Gregory M. Ferrence, and Lisa F. Szczepura

Department of Chemistry, Illinois State University, Normal, Illinois 61790-4160

Received May 16, 2003

Four azuliporphyrins, two *meso*-unsubstituted and two *meso*-tetraaryl substituted, were investigated in the synthesis of novel organometallic compounds. The *meso*-unsubstituted or "etio" series azuliporphyrins **8** reacted with nickel(II) acetate, palladium(II) acetate, and platinum(II) chloride in DMF to give the corresponding chelates **14**–**16**, where the metal cation lies within the macrocyclic cavity and binds to all three nitrogens and the internal carbon atom. The newly available *meso*-tetraarylazuliporphyrins **13** similarly afforded the corresponding nickel(II), palladium(II), and platinum(II) complexes, **17**–**19**, respectively. The new organometallic complexes are stable nonpolar compounds and were fully characterized spectroscopically and by mass spectrometry. The UV–vis data indicate that these complexes, in common with the parent azuliporphyrin system **8**, do not possess porphyrin-type aromaticity. However, electron donation from the azulene unit can give rise to dipolar resonance contributors that provide a degree of carbaporphyrin-type aromatic character. The platinum(II) azuliporphyrins **16** gave noteworthy proton NMR spectra where the *meso*-protons showed satellite peaks due to transannular coupling to platinum-195. The pyrrolic protons of the platinum(II) *meso*-tetraarylazuliporphyrin **19b** also showed similar satellite peaks due to coupling from the platinum-195 isotope. The electrochemistry of free base tetraphenylazuliporphyrin **13a** and the related nickel(II) and palladium(II) complexes was investigated using cyclic voltammetry, and these data indicate that metal coordination improves the reversibility of the ligand-based oxidations. Nickel(II) azuliporphyrin **14a** and palladium(II) tetrakis(4-chlorophenyl)azuliporphyrin **18b** were also structurally characterized by X-ray crystallography. The macrocyclic core of the palladium(II) complex **18b** was significantly more planar than the nickel(II) derivative **14b**, and this difference was attributed to the better size match between the azuliporphyrin cavity and the larger palladium(II) ion. The straightforward synthesis of metalloazuliporphyrins under mild conditions, and their interesting spectroscopic, electrochemical, and structural features, demonstrates that the azuliporphyrin system holds great promise as a platform for organometallic chemistry.

Introduction

The activation of C−H bonds toward metalation has important industrial applications and is a topic of great current interest.[1] In addition, stable organometallic systems may have unusual chemical and spectroscopic properties.[2] The N-confused porphyrins (NCPs; e.g., **1**)[2,3] have emerged as a superior system for generating organometallic derivatives under mild conditions, and these porphyrin isomers also show some promise in the stabilization of unusual oxidation states.[2,4] NCPs react as "dianionic ligands" (cross-conjugated tautomer **1a**, Chart 1) with nickel(II) or copper(II) acetate under mild conditions to generate the cross-conjugated metal(II) derivatives **2a** and **2b**.[5,6] Alternatively, NCPs can behave

* Author to whom correspondence should be addressed. E-mail: tdlash@ilstu.edu.

† Conjugated Macrocycles Related to the Porphyrins. 29. Part 28: Lash, T. D.; Colby, D. A.; Ferrence, G. M. *Eur. J. Org. Chem.*, in press.

(1) (a) Arndtsen, B. A.; Bergman, R. G.; Mobley, T. A.; Peterson, T. H. *Acc. Chem. Res.* **1995**, *28*, 154. (b) Shilov, A. E.; Shul'pin, G. B. *Chem. Rev.* **1997**, *97*, 2879.

(2) Furuta, H.; Maeda, H.; Osuka, A. *Chem. Commun.* **2002**, 1795.

(3) (a) Furuta, H.; Asano, T.; Ogawa, T. *J. Am. Chem. Soc.* **1994**, *116*, 767. (b) Chmielewski, P. J.; Latos-Grazynski, L.; Rachlewicz, K.; Glowiak, T. *Angew. Chem., Int. Ed. Engl.* **1994**, *33*, 779. (c) Liu, B. Y.; Brückner, C.; Dolphin, D. *Chem. Commun.* **1996**, 2141. (d) Geier, G. R., III; Haynes, D. M.; Lindsey, J. S. *Org. Lett.* **1999**, *1*, 1455. (e) Lash, T. D.; Richter, D. T.; Shiner, C. M. *J. Org. Chem.* **1999**, *64*, 7973.

(4) Furuta, H.; Ogawa, T.; Uwatoko, Y.; Araki, K. *Inorg. Chem.* **1999**, *38*, 2676.

10.1021/ic030166b CCC: $25.00
Published on Web 10/09/2003

Chart 1

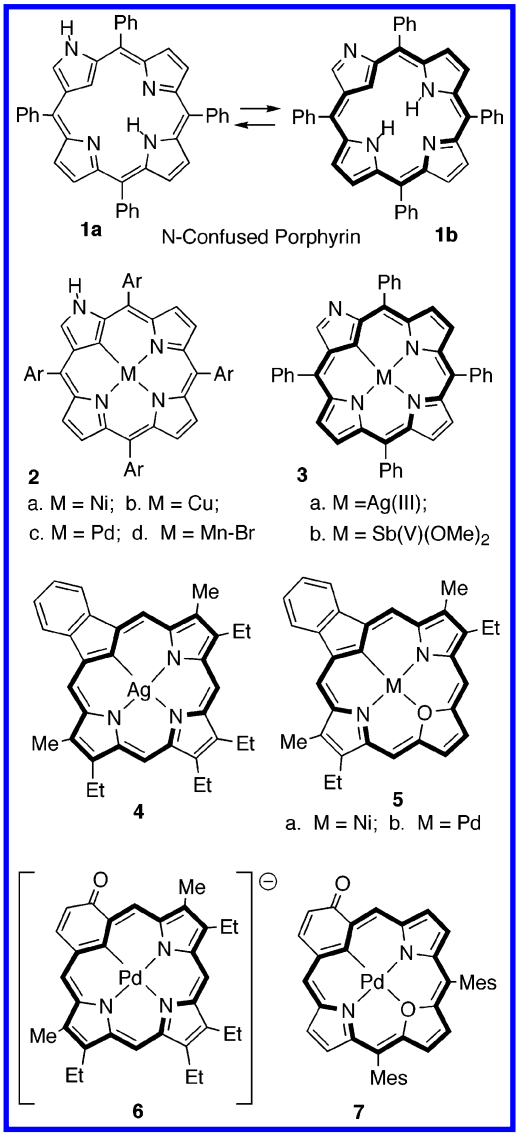

as "trianionic ligands" (fully aromatic tautomer **1b**) in reactions with silver(I) acetate to afford the silver(III) complex **3a**.[4] A similar antimony(V) complex **3b** with two axial methoxy ligands has also been reported.[7] Reaction of **1** with palladium(II) acetate can give the palladium(II) complex **2c**, but under some conditions dimeric products with additional C−Pd bonds to the phenyl substituents are produced.[8] Zinc acetate coordinates with the three nitrogens from the NCP core and a molecule of pyridine, but X-ray crystallography suggests that there is an additional side-on η^1-type interaction to the internal carbon atom.[9] Similar interactions can also be observed in a dimeric acetate derivative.[9] Anaerobic reaction of NCP **1** with ferrous bromide gave a complex with an agostic η^2 CH interaction,[10] while reactions with $MnBr_2$ gave a similar complex that readily oxidized to give the manganese(III) derivative **2d**.[11] Finally, $[Rh(CO)_2Cl]_2$ reacts with **1** to give inner core coordination of a Rh(I) at two of the interior nitrogens with outer core coordination to a second Rh(I) at the macrocyclic periphery.[12]

Given the wealth of organometallic and coordination chemistry that is associated with the NCPs,[2] it is surprising that related carbaporphyrinoid systems initially received very little attention.[13,14] However, organometallic derivatives of true carbaporphyrins (e.g., silver(III) derivatives **4**),[15,16] oxacarbaporphyrins (nickel(II) and palladium(II) complexes **5**),[17] oxybenziporphyrins (palladium derivatives, e.g., **6**),[18] oxaoxybenziporphyrins (palladium(II) complex **7**),[19] and benziporphyrins (palladium and platinum derivatives)[20] have recently been described. In addition, we have recently demonstrated that azuliporphyrins **8** possess a CNNN coordination core that is well suited to the production of related organometallic species.[21,22]

Azuliporphyrins **8** (Scheme 1) are porphyrin analogues where one of the pyrrole rings has been replaced by an azulene unit.[23,24] They are cross-conjugated systems, and for this reason the free base form does not exhibit the typical aromatic characteristics associated with the porphyrins.[23] The UV−vis spectra for azuliporphyrins do not show strong Soret bands near 400 nm, as would be expected for an aromatic system of the porphyrin family,[25] and only broad ill-defined

(5) Chmielewski, P. J.; Latos-Grazynski, L.; Schmidt, I. *J. Am. Chem. Soc.* **1996**, *118*, 5690.
(6) Chmielewski, P. J.; Latos-Grazynski, L.; Schmidt, I. *Inorg. Chem.* **2000**, *39*, 5475.
(7) Ogawa, T.; Furuta, H.; Morino, A.; Takahashi, M.; Uno, H. *Organomet. Chem.* **2000**, *611*, 551.
(8) (a) Furuta, H.; Kubo, N.; Maeda, H.; Ishizuka, T.; Osuka, A.; Nanami, H.; Ogawa, T. *Inorg. Chem.* **2000**, *39*, 5424. (b) Furuta, H.; Maeda, H.; Osuka, A.; Yasutake, M.; Shinmyozu, T.; Ishikawa, Y. *Chem. Commun.* **2000**, 1143.
(9) Furuta, H.; Ishizuka, T.; Osuka, A. *J. Am. Chem. Soc.* **2002**, *124*, 5622.
(10) Chen, W.-C.; Hung, C. H. *Inorg. Chem.* **2001**, *40*, 5070.
(11) Bohle, D. S.; Chen, W.-C.; Hung, C.-H. *Inorg. Chem.* **2002**, *41*, 3334.
(12) Srinivasan, A.; Furuta, H.; Osuka, A. *Chem. Commun.* **2001**, 1666.
(13) (a) Hayes, M. J.; Spence, J. D.; Lash, T. D. *Chem. Commun.* **1998**, 2409. (b) Lash, T. D.; Muckey, M. A.; Hayes, M. J.; Liu, D.; Spence, J. D.; Ferrence, G. M. *J. Org. Chem.*, in press.
(14) (a) Lash, T. D. *Synlett* **2000**, 279. (b) Lash, T. D. In *The Porphyrin Handbook*; Kadish, K. M., Smith, K. M., Guilard, R., Eds.; Academic Press: San Diego, **2000**; Vol. 2, pp 125−199.
(15) (a) Muckey, M. A.; Szczepura, L. F.; Ferrence, G. M.; Lash, T. D. *Inorg. Chem.* **2002**, *41*, 4840. (b) Lash, T. D.; Hayes, M. J.; Spence, J. D.; Muckey, M. A.; Ferrence, G. M.; Szczepura, L. F. *J. Org. Chem.* **2002**, *67*, 4860. (c) Liu, D.; Lash, T. D. *J. Org. Chem.* **2003**, *68*, 1755.
(16) Lash, T. D.; Colby, D. A.; Muckey, M. A.; Liu, D.; Ferrence, G. M. *Abstracts of Papers*, 225th National Meeting of the American Chemical Society, New Orleans, LA; American Chemical Society: Washington, DC, 2003; INOR 672.
(17) Liu, D.; Lash, T. D. *Chem. Commun.* **2002**, 2426.
(18) (a) Stepien, M.; Latos-Grazynski, L.; Lash, T. D.; Szterenberg, L. *Inorg. Chem.* **2001**, *40*, 6892. (b) Lash, T. D. *Angew. Chem., Int. Ed. Engl.* **1995**, *34*, 2533. (c) Lash, T.D.; Chaney, S. T.; Richter, D. T. *J. Org. Chem.* **1998**, *63*, 9076. (d) Richter, D. T.; Lash, T. D. *Tetrahedron* **2001**, *57*, 3659.
(19) Venkatraman, S.; Anand, V. G.; Pushpan, S. K.; Sankar, J.; Chandrashekar, T. K. *Chem. Commun.* **2002**, 462.
(20) Stepien, M.; Latos-Grazynski, L. *Chem. Eur. J.* **2001**, *7*, 5113.
(21) Preliminary communication: Graham, S. R.; Ferrence, G. M.; Lash, T. D. *Chem. Commun.* **2002**, 894.
(22) These results were presented, in part, at the following meetings: (a) 221st National Meeting of the American Chemical Society, San Diego, CA, April 2001 (Graham, S. R.; Lash, T. D. *Abstracts of Papers*, ORGN 186); (b) 2nd International Conference on Porphyrins and Phthalocyanines (ICPP-2), Kyoto, Japan, July 2002 (Lash, T. D. *Book of Abstracts*, Abstract No. S-76); (c) 225th National Meeting of the American Chemical Society, New Orleans, LA, March 2003 (Lash, T. D.; Colby, D. A.; Graham, S. R.; Ferrence, G. M. *Abstracts of Papers*, INOR 673).
(23) Lash, T. D.; Chaney, S. T. *Angew. Chem., Int. Ed. Engl.* **1997**, *36*, 839.
(24) Lash, T. D. *Chem. Commun.* **1998**, 1683.

Scheme 1

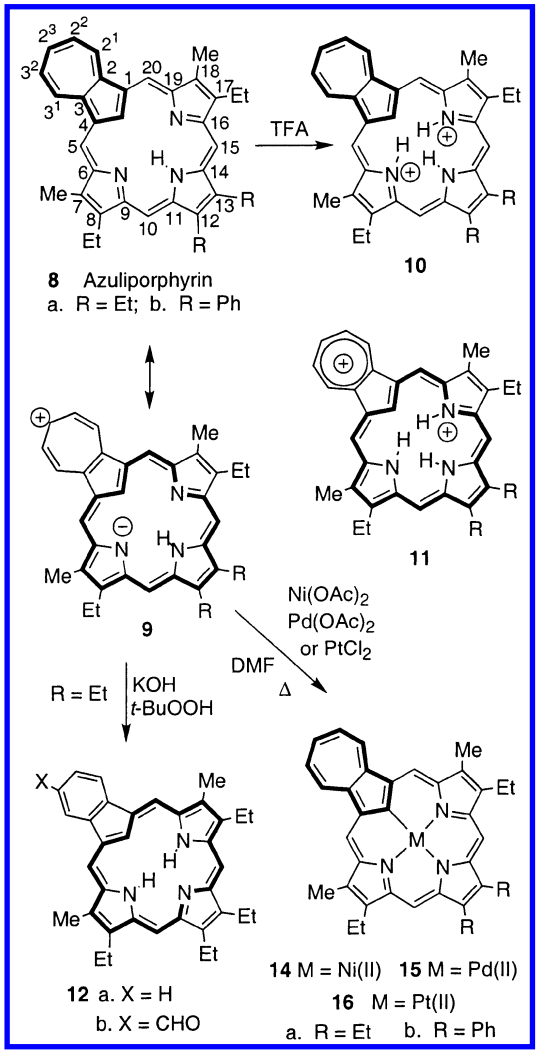

absorptions are observed through the visible region instead of porphyrin-type Q bands.[23] On the other hand, the proton NMR spectrum for **8** in $CDCl_3$ gave resonances for the two types of *meso*-protons that were somewhat shifted downfield to ca. 8.0 and 9.0 ppm.[23] While these values are nowhere near the shifts observed for true porphyrins, which show these resonances near 10 ppm, the data suggest that azuliporphyrins have a significant diatropic ring current.[14] In addition, this proposal is supported by the observation that the internal CH resonates upfield at +1.5 ppm, although this is a pale shadow of the shifts observed for aromatic carbaporphyrins where the CH resonance is commonly seen at −7 ppm.[25] The weak diatropic character observed for **8** was attributed to contributions from dipolar resonance forms such as **9** that simultaneously give the structure 18π electron aromatic character and external tropylium characteristics.[23] Nonetheless, this contribution is limited due to the associated charge separation which restricts the degree of aromatic character for azuliporphyrins. However, addition of acid "switches on" a strong diatropic ring current by generating a diprotonated dication **10** that favors charge delocalization through analogous tropylium-fused carbaporphyrin forms as illustrated by the hybrid structure **11**.[23] In TFA−$CDCl_3$, the proton NMR spectrum of **8** shows the *meso*-protons at 9.42 and 9.95 ppm, while the interior CH resonates at −2.56 ppm.[23] The UV−vis spectrum of the dication also becomes substantially more porphyrin-like showing two Soret-like absorptions at 364 and 460 ppm.[23]

Azuliporphyrins **8** can easily be synthesized by two different versions of the MacDonald "3 + 1" condensation.[23,26,27] The azuliporphyrin system was first reported by our group in 1997[23] and has been shown to have unique chemical properties, specifically in its ability to undergo an oxidative ring contraction to afford benzocarbaporphyrins **12** (Scheme 1).[24] Recently, we also reported a one-pot synthesis of *meso*-tetraarylazuliporphyrins from azulene, pyrrole, and arylaldehydes under Lindsey-type Rothemund reaction conditions.[28−30] This chemistry makes the azuliporphyrin system readily available for the first time and has facilitated more detailed studies into the chemistry of these important porphyrin analogues. In this paper, we report full details on the synthesis and spectroscopy of nickel(II), palladium(II), and platinum(II) azuliporphyrins.[21,22] In addition, structural characterizations of two organometallic derivatives and preliminary electrochemical studies have been performed.

Results and Discussion

The cross-conjugated azuliporphyrin system structurally resembles the nonaromatic tautomer **1a** of the N-confused porphyrins[31] and for this reason might be expected to undergo similar metal insertion reactions. Indeed, shortly after we first reported the synthesis of azuliporphyrin **8a**, Ghosh and co-workers performed a DFT study on this system and noted that it should be well suited for metalation.[32] Initially, we reacted azuliporphyrin **8a** with nickel(II) acetate in refluxing chloroform−methanol, but this produced only low yields of the related nickel(II) complex **14a**. However, when the chemistry was carried out in DMF at 80−90 °C, **14a** was produced in good yields after 10 min. Following chromatography on silica gel eluting with chloroform, and crystallization from chloroform−hexanes, the chelate was isolated in 64% yield. The metallo derivative was stable to air and water, and was relatively nonpolar as judged by TLC (R_f value) and column chromatography compared to the free base azuliporphyrin **8a**. The diphenyl porphyrinoid **8b** reacted similarly to give the nickel(II) complex in 73% yield. Both metal complexes gave complex UV−vis spectra (Figure 1A) showing a moderately strong band at 385 nm in the case of

(25) Lash, T. D.; Hayes, M. J. *Angew. Chem., Int. Ed. Engl.* **1997**, *36*, 840.

(26) Lash, T. D. *Chem. Eur. J.* **1996**, *2*, 1197.
(27) Graham, S. R.; Colby, D. A.; Lash, T. D. *Angew. Chem., Int. Ed.* **2002**, *41*, 1371.
(28) Colby, D. A.; Lash, T. D. *Chem. Eur. J.* **2002**, *8*, 5397.
(29) Colby, D. A.; Lash, T. D. *Book of Abstracts for the 2nd International Conference on Porphyrins and Phthalocyanines (ICPP-2)*, Kyoto, Japan, June 30 to July 5, 2002; Abstract No. P-247.
(30) See also: Colby, D. A.; Lash, T. D. *J. Org. Chem.* **2002**, *67*, 1031.
(31) Furuta, H.; Ishizuka, T.; Osuka, A.; Dejima, H.; Nakagawa, H.; Ishikawa, I. *J. Am. Chem. Soc.* **2001**, *123*, 6207.
(32) Ghosh, A.; Wondimagegn, T.; Nilsen, H. J. *J. Phys. Chem. B* **1998**, *102*, 10459.

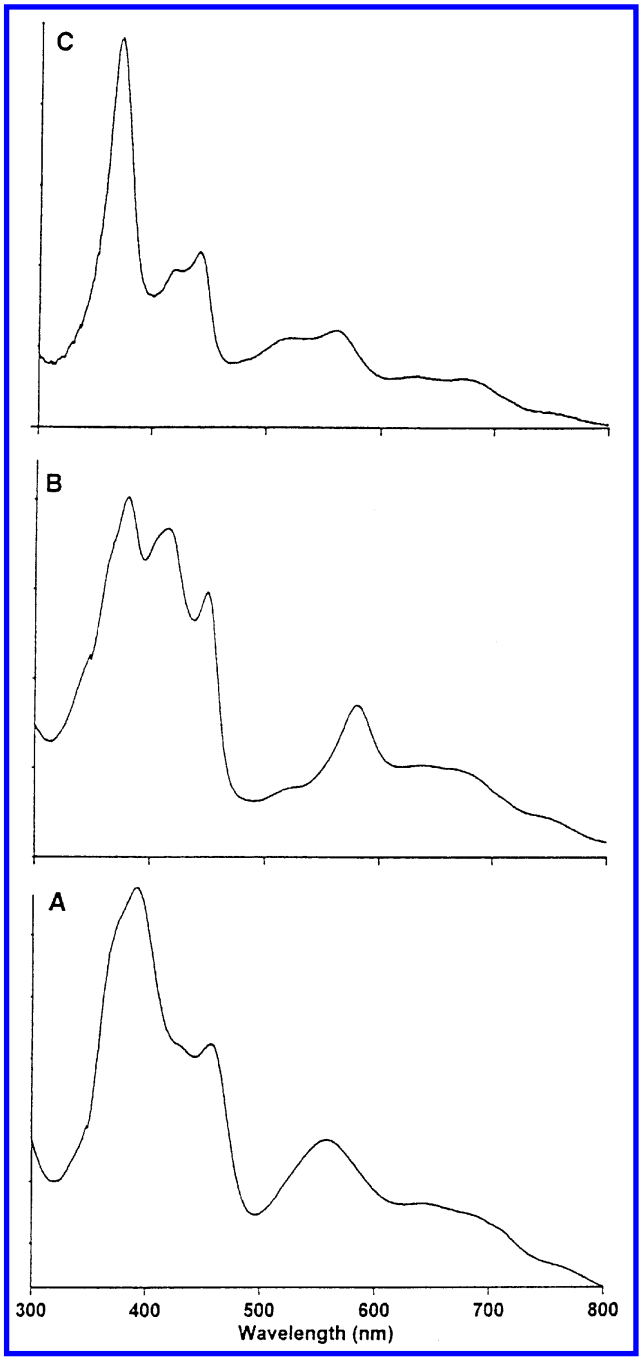

Figure 1. UV−vis absorption spectra of metalloazuliporphyrins in chloroform: (A) nickel(II) complex **14b**; (B) palladium(II) complex **15b**; (C) platinum(II) complex **16b**.

14a and broad absorptions through the visible region. The nickel(II) diphenylazuliporphyrin **14b** showed slightly red shifted absorptions but otherwise closely resembled **14a** by UV−vis spectroscopy. Mass spectrometry confirmed that nickel had been incorporated into the macrocycle, and the spectroscopic data were fully consistent with the proposed organometallic derivatives **14**. Nickel complex **14a** was only sparingly soluble, but it was possible to obtain a proton NMR spectrum in $CDCl_3$. The *meso*-protons were observed as two 2H singlets at 8.5 and 9.1 ppm, values that are slightly downfield from those reported for free base azuliporphyrin **8a** in $CDCl_3$. These resonances showed considerable broadening, possibly due to aggregation in solution, although the *meso*-protons were much better resolved at higher temperatures. However, the *meso*-protons for **14a** in d_5-pyridine gave sharp, well-resolved resonances that were further shifted downfield to give values of 8.9 and 9.6 ppm (the analogous resonances for **8a** in d_5-pyridine were previously observed at 8.6 and 9.5 ppm[23]). In addition, the porphyrinoid methyl groups in **14a** gave rise to a 6H singlet at 3.07 ppm, which compares to values for **8a** of 3.0 ppm in $CDCl_3$ and 3.1 ppm in d_5-pyridine. Pyridine may aid in stabilizing the dipolar canonical forms for azuliporphyrins and their metallo derivatives and thereby enhance the diatropic character for this system. In any case, the data indicate that the degree of macrocyclic aromaticity in **14a** is slightly enhanced compared to the parent system **8a**. Similar results were obtained for the diphenyl-substituted azuliporphyrin chelate **14b**. However, this latter derivative was more soluble and this allowed the carbon-13 NMR spectrum to be obtained. Unfortunately, as is the case for all of the reported metalloazuliporphyrins in this paper, we were unable to identify the internal carbon in the carbon-13 NMR spectra. However, the data does demonstrate that the macrocycle has a plane of symmetry and the two types of *meso*-carbons gave resonances at 99.9 and 108.5 ppm, values that are similar to those observed for the free base azuliporphyrins **8**.

Palladium(II) acetate was found to react with azuliporphyrins **8** under the same conditions to afford the related palladium(II) derivatives **15**. The UV−vis spectra of the palladium chelates (Figure 1B) were quite different from the nickel complexes **14** and showed three bands in the range of 360−450 nm, together with broad absorptions from 500 to 800 nm. As was the case for the nickel(II) complexes, the diphenyl derivative **15b** showed small bathochromic shifts compared to **15a**. The palladium(II) complexes were also only sparingly soluble in $CDCl_3$, and the proton NMR spectra for **15** in this solvent gave highly broadened resonances for the *meso*-protons. Again, these signals sharpened up somewhat at higher temperatures. In addition, the proton NMR spectrum of **15a** in d_5-pyridine showed the *meso*-protons as two well-defined 2H singlets at 9.02 and 9.78 ppm, values that suggest a further enhancement of the macrocyclic ring current in the palladium chelates compared to **8** and **14**. This hypothesis is further supported by the observation that the porphyrinoid methyl units are also shifted slightly downfield to 3.2 ppm (6H, s). We speculate that the palladium(II) ion is a better fit for the macrocyclic cavity and this allows the azuliporphyrin to take on a more planar conformation for **15** compared to **14**. Structural evidence to support this proposal is provided below. As was the case for the nickel(II) chelates, carbon-13 NMR data could only be obtained for the diphenyl-substituted azuliporphyrin complex **15b**. This confirmed the presence of a plane of symmetry and showed the *meso*-carbons at 100.7 and 110.7 ppm. High-resolution mass spectrometry also confirmed the molecular formulas for these organometallic species.

Reaction of **8a** or **8b** with platinum(II) chloride gave lower yields (23−27%) of the platinum(II) complexes **16**. The best results were still obtained in DMF, and reactions in ben-

zonitrile afforded only low yields of the metalloporphyrinoids. The UV−vis spectra for the platinum(II) derivatives **16** (Figure 1C) were rather different from the nickel(II) or palladium(II) complexes showing a strong band at 367 nm for **16a**, and 372 nm for **16b**, together with a series of broad ill-defined absorptions from 400 to 800 nm. Once again, the bands for the diphenyl derivative **16b** were shifted to slightly longer wavelengths than **16a**. A closer examination of the UV−vis spectra for **14**, **15**, and **16** (Figure 1) indicates that the same absorptions are present in each case, but they nonetheless vary considerably in broadness and relative intensity. The proton NMR spectrum for **16a** in $CDCl_3-d_5$-pyridine showed the *meso*-protons at 8.86 and 9.37 ppm, values that suggest a slight decrease in the overall aromaticity compared to **14a** and **15a**. The NMR spectra for both **16a** and **16b** showed satellite peaks for the *meso*-protons (Figure 2) due to coupling from the isotope platinum-195 (natural abundance 33.8%). This transannular coupling constant is significant falling into the range of 4.4−5.6 Hz. The $^4J_{Pt,H}$ values for the 5,20-protons were consistently ca. 25% larger than those for the 10,15-protons. Due to solubility problems, only a poor quality carbon-13 NMR spectrum could be obtained for **16b**, but this showed values for the *meso*-carbons (98.6, 110.3) similar to those reported above for **14b** and **15b**.

Attempts to react azuliporphyrins **8** with silver(I) acetate in refluxing DMF gave low yields of silver(III) carbaporphyrins. In control experiments, azuliporphyrins **8** were found to slowly produce benzocarbaporphyrins **12** in refluxing DMF, although not in synthetically useful yields, and silver(I) acetate does not appear to play a significant role in producing the ring-contracted products. As carbaporphyrins have previously been shown to incorporate silver(III) ions in reactions with silver(I) acetate, the formation of silver(III) carbaporphyrins is to be expected.[15] Reactions of **8** with copper(II) acetate also readily produce metallo derivatives, but in this case the chemistry is not straightforward and further investigations will be required.

Recently, we reported a straightforward methodology for synthesizing *meso*-tetraarylazuliporphyrins **13** (Scheme 2).[28,29] The availability of these new *meso*-substituted porphyrinoids has allowed us to extend the metalation chemistry, specifically to the tetraphenyl- and tetrakis(4-chlorophenyl)azuliporphyrins **13a** and **13b**, respectively. Azuliporphyrins **13** reacted with nickel(II) or palladium(II) acetate in DMF to give the metallo derivatives **17** and **18** in 65−97% yield. Platinum(II) chloride also reacted with azuliporphyrins **13** but, as had been the case in the *meso*-unsubstituted series, the related platinum(II) chelates could only be isolated in relatively poor yields (22−23%). The UV−vis spectra for the metallo derivatives were quite varied (Figure 3), and also differed somewhat from their *meso*-unsubstituted counterparts **14**−**16** as well. The tetraphenyl and tetrakis(4-chlorophenyl) series of metalloporphyrinoids showed very similar UV−vis spectra, and only the latter "**b**" series will be discussed in this section. Nickel(II) complex **17b** gave a strong band at 400 nm, two broader absorption at 473 and 490 nm, and weaker broadened bands from 590 to 800 nm.

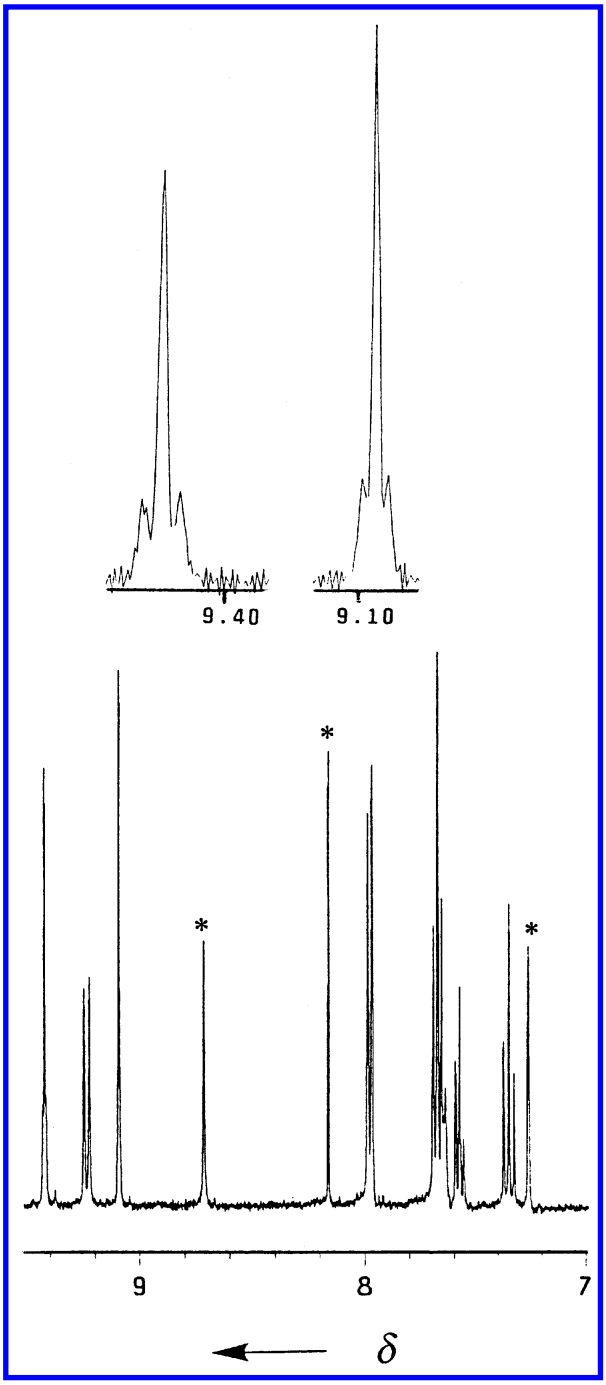

Figure 2. Partial 400 MHz proton NMR spectrum of the downfield region for the platinum(II) azuliporphyrin **16b** in d_5-pyridine−$CDCl_3$. The *meso*-proton resonances at 9.09 and 9.43 ppm have been expanded to show the ^{195}Pt satellite peaks. Signals labeled with an asterisk (*) correspond to solvent impurities.

In contrast, palladium(II) derivative **18b** gave three strong bands at 374, 403, and 482 nm, and weaker broad bands between 580 and 800 nm. The platinum(II) complex **19b** more closely resembled the nickel complex, showing a strong band at 383 nm, two weaker bands at 444 and 466 nm, and the same type of weaker broadened absorptions from 560 to 800 nm. The platinum(II) complexes **19** gave UV−vis spectra that more closely resembled their "etio" counterparts **16** than was the case for the nickel(II) or palladium(II) complexes.

Scheme 2

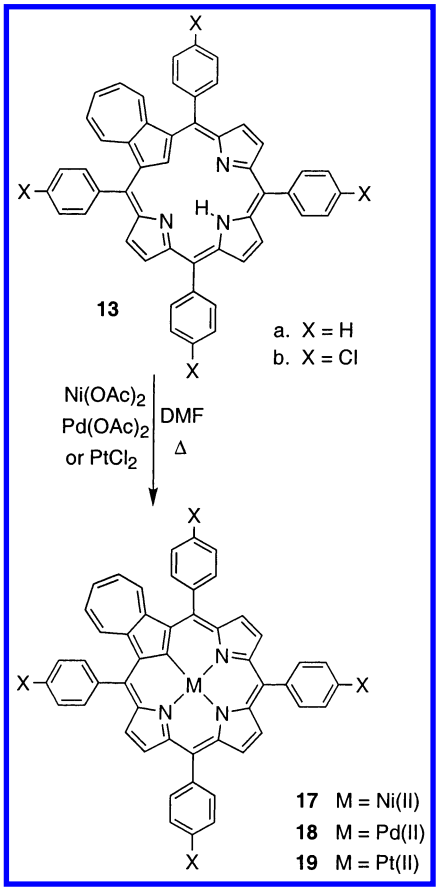

The proton NMR spectra for the tetrakis(4-chlorophenyl)-azuliporphyrin complexes **17b**, **18b**, and **19b** (Figure 4) were far better resolved than the corresponding tetraphenylazuliporphyrin derivatives, and for this reason the data for the "**b**" series will be discussed in detail. The nickel(II) complex in $CDCl_3$ showed the *meso*-protons as a 2H singlet at 7.97 ppm and two 2H doublets at 8.02 and 7.8 ppm (the latter overlaps with the resonances due to the *ortho*-protons on the aryl substituents). For the palladium(II) complex **18b**, these values are observed at 7.97, 8.04, and 7.92 ppm, while the platinum(II) derivative showed these resonances at 7.99, 7.94, and 7.91. The values fall too close together to make any real distinctions between the diatropic character for these chelates. However, the azulene protons vary to a greater extent. Nickel(II) complex **17b** gives a 2H triplet at 6.91, a 1H triplet at 7.21, and a 2H doublet at 7.43 ppm. These resonances are observed at 6.84, 7.16, and 7.45 ppm for **18b**, while the platinum(II) complex **19b** gives values of 6.66, 7.26, and 7.43 ppm. The 1H triplet should provide the best indication of the electronic character for the azulene unit, as the 2^3-proton is furthest removed from the remaining porphyrinoid π-system. These data indicate that the platinum complex takes on the greatest amount of tropylium character, while the palladium derivative has the least. However, it is worth noting that the 2H azulene triplet in the platinum complex is shifted the most upfield to 6.62 ppm, possibly indicating that the conformation of **19b** induces a greater amount of shielding at this position due to the orientation of the adjacent aryl substituent. The pyrrolic protons for the

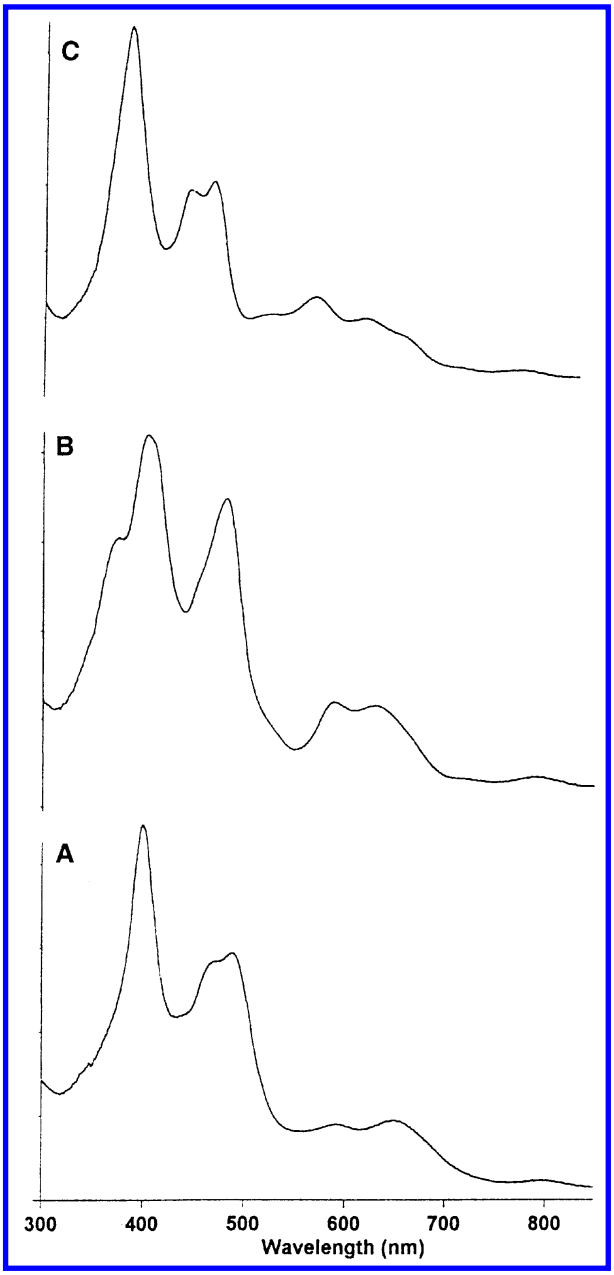

Figure 3. UV−vis absorption spectra of tetrakis(4-chlorophenyl)azuliporphyrin chelates in chloroform: (A) nickel(II) complex **17b**; (B) palladium(II) complex **18b**; (C) platinum(II) complex **19b**.

platinum(II) complex also show satellite peaks due to coupling from platinum-195. Again the coupling constants for this transannular interaction are significant (ca. 5 Hz).

In order to gain further insights into the properties of these metallo derivatives, preliminary electrochemical studies were conducted on the free base tetraphenylazuliporphyrin **13a** and its nickel(II) and palladium(II) derivatives, **17a** and **18a**, respectively. The cyclic voltammogram of **13a** is shown in Figure 5; this scan was initiated at the open circuit potential and scanned between the limits of −1.9 and +1.5 V vs Ag/$AgNO_3$. Starting at −0.4 V and scanning in the negative direction, there are two quasi-reversible cathodic waves at $E_{1/2} = -1.15$ and −1.68 V. After switching the potential at −1.9 V and continuing to scan in a positive direction, five oxidative waves, one irreversible wave at $E_{p,a} = -0.24$ V

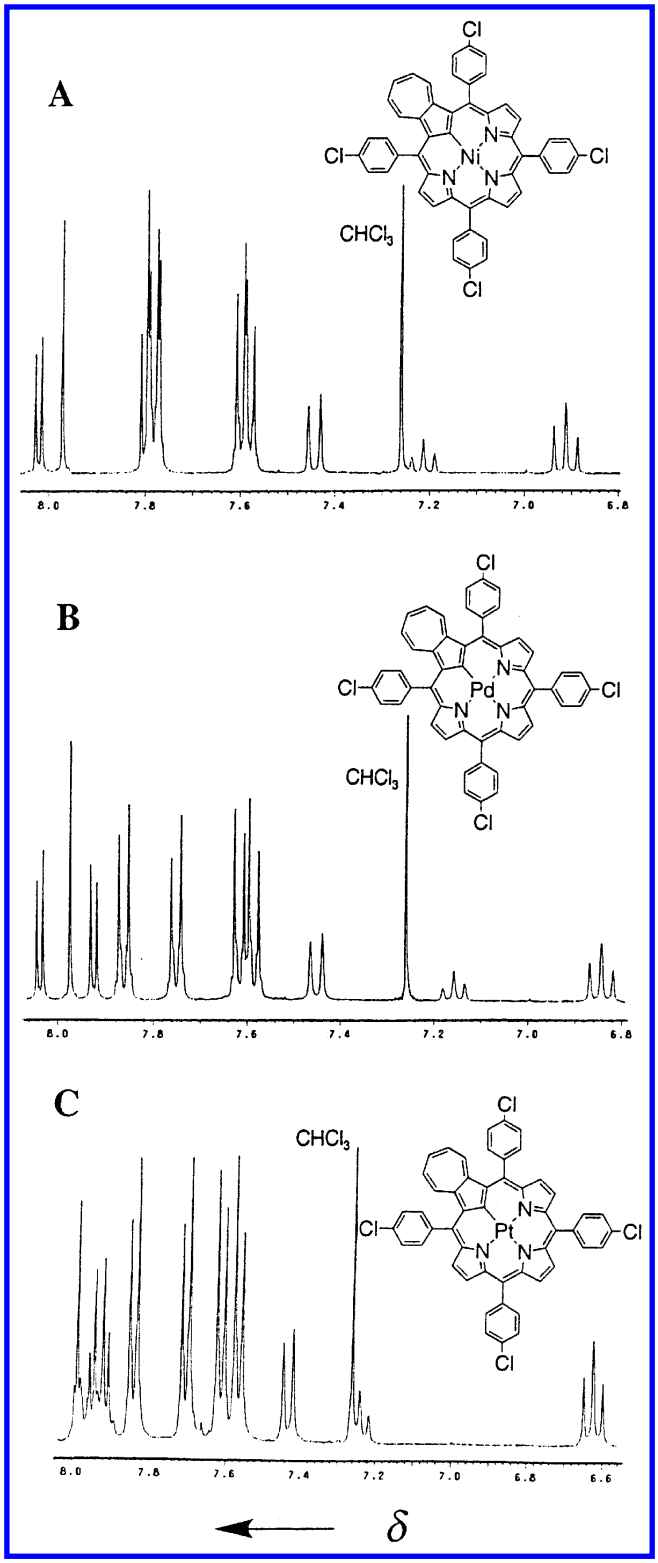

Figure 4. 400 MHz proton NMR spectrum of tetrakis(4-chlorophenyl)-azuliporphyrin chelates in $CDCl_3$: (A) nickel(II) complex **17b**; (B) palladium(II) complex **18b**; (C) platinum(II) complex **19b**. In the spectrum for **19b**, the ^{195}Pt satellite peaks for the pyrrolic protons are clearly evident between 7.9 and 8.0 ppm.

and four quasi-reversible waves at $E_{1/2} = +0.34$, $+0.70$, $+0.96$, and $+1.30$ V, are observed (scanning out further to $+1.7$ V did not reveal any additional waves). Switching potential experiments verified that the irreversible oxidative wave ($E_{p,a} = -0.24$ V) is only observed after scanning

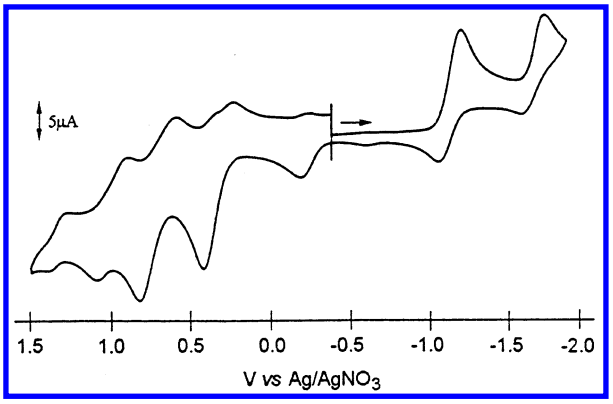

Figure 5. Cyclic voltammogram (200 mV/s) of **13a** in anhydrous dichloromethane, 0.2 M Bu_4NBF_4.

through the reductive wave at -1.68 V, indicating that it must be due to a decomposition product. While the first two oxidative waves look irreversible in Figure 5, they appear as quasi-reversible waves when scanning was started at -0.4 V and reversed at $+1.0$ V, instead of $+1.7$ V. Notably, the cyclic voltammogram of **13a** is similar to that of the previously reported free base carbaporphyrin **12a**[15b] in that both display more complex redox behavior than the well studied H_2TPP and H_2OEP.[33] Specifically, both **13a** and **12a** contain two reductive waves and numerous oxidative waves.[15b] However, there are also some significant differences between **13a** and **12a**, as would be expected for these rather different carbaporphyrinoid systems (for instance, **12a** shows a far greater degree of aromatic character than **13a**). (1) The difference between the two reductive waves of **13a** is $\Delta E_{1/2} = 0.53$ V, which is larger than the difference between the reductive waves for porphyrins and metalloporphyrins ($\Delta E_{1/2} = 0.42 \pm 0.05$ V) and for the free base carbaporphyrin **12a** ($\Delta E_{1/2} = 0.35$ V).[15b] (2) All of the oxidative waves in **13a** appear to be quasi-reversible, which is not the case for **12a**. (3) The HOMO−LUMO gap for **13a** is $E_{1/2}^{ox} - E_{1/2}^{red} = 1.49$ V, whereas the gap for carbaporphyrin **12a** is $E_{1/2}^{ox} - E_{1/2}^{red} = 2.17$ V. The HOMO−LUMO gap has been shown to be dependent on a variety of factors including the substituents on the ring and the planarity of the ring, so given the differences in aromatic character between **13a** and **12a** it is not surprising that these values are different.

The cyclic voltammogram of palladium(II) complex **18a** displays one irreversible reductive wave at $E_{p,c} = -1.15$ V, one irreversible oxidative wave at -0.14 V, and two reversible oxidative waves at $E_{1/2} = +0.46$ and $+1.01$ V when scanned in a similar manner as **13a** (Figure 6a). Switching potential experiments show that the $E_{p,a}$ at -0.14 V appears only after scanning through the reductive couple at -1.15 V. Therefore, this peak is assigned to a decomposition product. Only a few studies that focus on the electrochemistry of palladium porphyrin complexes have been reported to date.[33] Of these, Pd(TPP) and Pd(OEP) were reported to contain four waves: two reversible reductive waves and two reversible oxidative waves. We observed two

(33) Kadish, K. M.; van Caemelbecke, E.; Royal, G. In *The Porphyrin Handbook*; Kadish, K. M., Smith, K. M., Guilard, R., Eds.; Academic Press: San Diego, 2000; Vol. 8, pp 1−114.

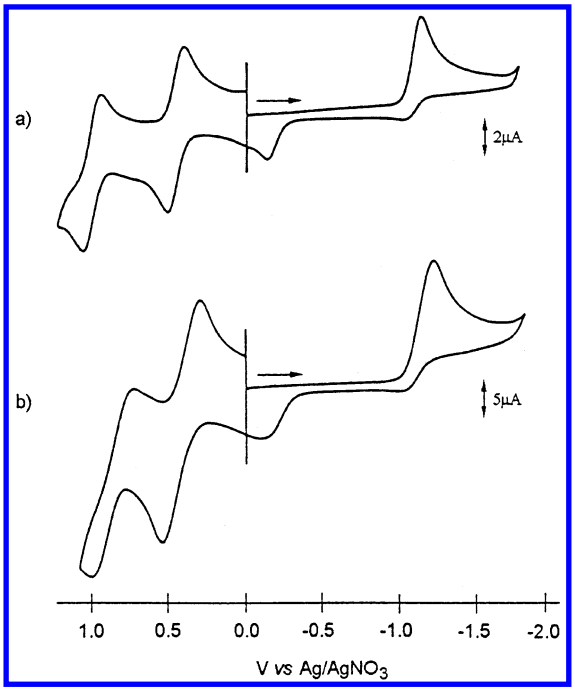

Figure 6. Cyclic voltammograms (200 mV/s) of the Pd (a, **18a**) and Ni (b, **17a**) complexes of azuliporphyrin in anhydrous dichloromethane, 0.2 M Bu_4NBF_4.

oxidative waves, but only one reductive wave within the limits scanned (+1.7 V to −1.9 V vs $Ag/AgNO_3$). The ΔE_p for the reversible processes are comparable to the ΔE_p of ferrocene run under similar conditions, indicating that these are one-electron processes. The difference between the oxidative waves of **18a** ($\Delta E_{1/2} = 0.55$ V) is within the range observed for Pd(TPP) ($\Delta E_{1/2} = 0.42$ V) and Pd(OEP) ($\Delta E_{1/2} = 0.72$ V). The HOMO−LUMO gap for **18a** ($E_{1/2}^{ox} - E_{1/2}^{red} = 1.61$ V) is much smaller than that for Pd(TPP) and Pd(OEP) ($E_{1/2}^{ox} - E_{1/2}^{red} \sim 2.4$ V). However, it is comparable to the gap for **13a**. In the case of the previously reported palladium porphyrin complexes, all waves have been unambiguously assigned to processes associated with the porphyrin ring itself. On the basis of the similarities between the cyclic voltammograms of **13a**, **18a**, and **17a** (i.e., the potentials for the oxidative and reductive processes as well as the HOMO−LUMO gap are comparable), and on the basis of the fact that oxidation to palladium(III) is unlikely, we propose that the couples observed in the cyclic voltammogram of **18a** are also ligand-centered redox processes.

The cyclic voltammogram of the analogous nickel(II) complex (**17a**) is similar to the palladium(II) complex **18a** in that it also shows one irreversible reductive wave at $E_{p,c} = -1.21$ V, one irreversible oxidative wave at $E_{p,a} = -0.19$ V, and two reversible oxidative waves at $E_{1/2} = +0.41$ and +0.86 V when it is scanned within the limits of −1.9 and +1.1 V (Figure 6b). As with the palladium(II) complex, the irreversible oxidative wave at $E_{p,a} = -0.19$ V is assigned to a decomposition product generated during the irreversible reduction. However, when the positive switching potential was increased to +1.7 V, two additional irreversible oxidative waves at $E_{p,a} = 1.45$ and 1.60 V are also observed (accessing these waves makes the waves at $E_{1/2} = 0.41$ and 0.86 V appear irreversible). Notably, the HOMO−LUMO gap of **17a** ($E_{1/2}^{ox} - E_{1/2}^{red} = 1.62$ V) is also similar to the free base azuliporphyrin **13a**. Due to the fact that the nickel(II) center can be oxidized to nickel(III) or reduced to nickel(I) within a narrow potential range, the electrochemical studies of nickel porphyrin complexes are more complex than those of palladium. Numerous studies focusing on the electrochemistry of nickel porphyrin complexes have been reported, and many have incorporated spectroscopic studies to help investigate the nature of the oxidized and reduced products.[33,34] We have not collected any spectro-electrochemical data. However, we do believe that the reversible waves at $E_{1/2} = 0.41$ and 0.86 V are ligand-centered oxidations, on the basis of the fact that these waves do not shift dramatically compared to the palladium(II) complex **18a** or the free base azuliporphyrin **13a**. Thus, we propose that at least one of the additional oxidative waves seen in the cyclic voltammogram of **17a** is due to a metal-centered redox process, i.e., a Ni(III)/(II) couple. These assignments are consistent with previous electrochemical reports on nickel(II) porphyrin complexes.

It is interesting to note that metal coordination by **13a** appears to improve the reversibility of the ligand-based oxidations. This is not the case with H_2TPP and H_2OEP where all four redox processes (two oxidative and two reductive) are reversible before and after metal coordination. The loss of protons upon coordination is likely to be partially responsible for increasing the reversibility of the oxidation couples in **17a** and **18a**. However, the proposed increase in aromatic character for the metal complexes compared to the free base azuliporphyrins may also be affecting the reactivity of the oxidized metal complexes.

Further insights into the structures of nickel(II) azuliporphyrin **14b** and palladium(II) tetrakis(4-chlorophenyl)azuliporphyrin **18b** were obtained by single-crystal X-ray diffraction analysis. Both represent the first structurally characterized azuliporphyrin complexes. Crystal data and a summary of the intensity data and collection parameters for these structures are given in Table 1, and ORTEP III illustrations and selected bond lengths and angles summarizing the coordination spheres of the metals are given in Figures 7 and 8.

In the case of **14b**, the macrocycle is significantly distorted from planarity (Figure 7) as evidenced by the pyrrole to mean [18]annulene plane dihedral angles of 14.3(1)°, 16.8(1)°, and 19.9(1)°, and the azulene to mean [18]annulene plane dihedral angle of 15.0(1)°. The nickel(II) ion is essentially situated over the center of the macrocyclic cavity and draws the macrocycle into a bowl with the nickel atom slightly above the C(21), N(22), N(23), N(24) plane. The dihedral angle between the azulene plane and the pyrrole N(23) plane is 34.8(1)°, and the dihedral angle between the pyrrole N(22) and pyrrole N(24) planes is 30.8(2)°. These parameters in conjunction with the distances (0.327 Å rms) at which skeletal atoms lie from the plane defined by Ni(1)C(21)N-

(34) (a) Kadish, K. M.; Sazou, D.; Maiya, G. B.; Han, B. C.; Liu, Y. M.; Saoiabi, A.; Ferhat, M.; Guilard, R. *Inorg. Chem.* **1989**, *28*, 2542. (b) Connick, P. A.; Macor, K. A. *Inorg. Chem.* **1991**, *30*, 4654.

Table 1. Summary of the Crystal Structure Data Collection and Refinement for **14b** and **18b**

	14b	**18b**
chemical formula	$C_{44}H_{35}N_3Ni$	$C_{50}H_{27}Cl_4N_3Pd \cdot {}^7/_6(CHCl_3)$
M_r, g/mol	664.5	1049.25
crystal system	monoclinic	triclinic
space group	$P2_1/n$	$P\bar{1}$
unit cell params		
a, Å	31.028(2)	12.4999(8)
b, Å	8.8409(6)	13.4732(9)
c, Å	11.7434(8)	14.949(1)
α, deg		71.939(1)
β, deg	96.166(2)	89.423(1)
γ, deg		68.782(1)
V, Å^3	3202.8(4)	2216.4(3)
Z	4	2
D_{calcd}, Mg m^{-3}	1.378	1.581
μ, mm^{-1}	0.644	0.912
T, K	193(2)	193(2)
reflns collected	14860	12937
indep reflns	6534	8946
reflns obsd	4718 ($I > 2\sigma_I$)	7795 ($I > 2\sigma_I$)
θ range, deg	1.8−26.4	1.72−26.39
$R[F^2 > 2\sigma(F^2)]$	0.052	0.0395
$wR(F^2)$ observed	0.116	0.0994
S	1.009	1.032
params (restraints)	433 (0)	575 (6)

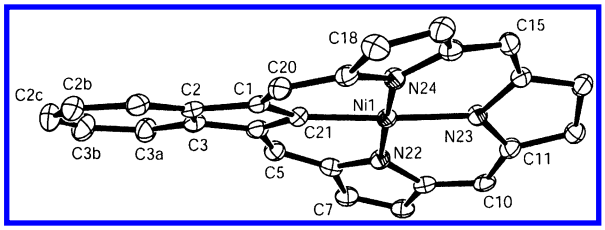

Figure 7. ORTEP III drawing (50% probability level) of **14b**, depicting the presence of a ruffled conformation; hydrogen atoms and core substituents have been omitted for clarity. Selected bond lengths (Å): C(21)−Ni 1.896(3), N(22)−Ni 1.934(2), N(23)−Ni 1.964(2), N(24)−Ni 1.928(2), C(1)−C(21) 1.417(4), C(4)−C(21) 1.426(4). Selected bond angles (deg): C(21)−C(1)−C(2) 110.6(3), C(1)C(2)−C(3) 106.5(3), C(2)−C(3)−C(4) 106.8(3), C(3)−C(4)−C(21) 110.6(3), C(4)−C(21)−C(1) 105.3(2), C(6)−N(22)−C(9) 104.7(2), C(11)−N(23)−C(14) 105.3(2), C(16)−N(24)−C(19) 104.6(2), C(21)−Ni−N(22) 90.4(1), N(22)−Ni−N(23) 90.1(1), N(23)−Ni−N(24) 89.9(1), N(24)−Ni−C(21) 89.9(1), C(21)−Ni−N(23) 177.2(1), N(22)−Ni−N(24) 176.2(1).

(22)N(23)N(24) classify the porphyrin skeleton as ruffled. Particularly illustrative are the C(5), C(10), C(15), and C(20) bridges which alternate being above and below the plane and exhibit four of the five largest deviations from the plane at −0.424(3), 0.503(3), −0.474(3), and 0.502(3) Å, respectively. In the context of this discussion, *cis* and *trans* notations are relative to the carbon atom bonded to the metal. The metal is centered between the donor ligands with equivalent *cis*-Ni−N bond lengths of 1.934(3) and 1.928(3) Å. These values fall within the typical 1.924 ± 0.025 Å range reported for ruffled nickel(II) coordinated porphyrin-type macrocycles.[35] The shorter Ni(1)−C(21) bond length of

(35) Bruno, I. J.; Cole, J. C.; Edgington, P. R,; Kessler, M.; Macrae, C. F.; McCabe, P.; Pearson, J.; Taylor, R. *Acta Crystallogr.* **2002**, *B58*, 389. A search of the Cambridge Structural Data base query returned 198 hits for tetrapyrrole nickel complexes with CR bridges at the α carbons. These hits were broadly sorted into ruffled (169) and planar (29) populations; comparison was made to the 211 Ni−N (nickel to pyrrole) distances averaged from the ruffled population. A CSD search returned 11 hits for tetrapyrrole palladium complexes with CR bridges at the α carbons; from these hits 60 Pd−Ni (palladium to pyrrole) distances were averaged.

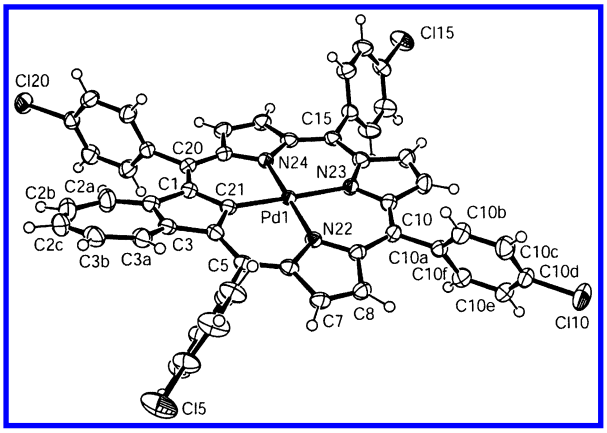

Figure 8. ORTEP III drawing (50% probability level) of **18b**, depicting the planar conformation with hydrogen atoms drawn arbitrarily small. Selected bond lengths (Å): C(21)−Pd 1.980(3), N(22)−Pd 2.021(2), N(23)−Pd 2.075(2), N(24)−Pd 2.016(2), C(1)−C(21) 1.427(4), C(4)−C(21) 1.436(4). Selected bond angles (deg): C(21)−C(1)−C(2) 108.9(2), C(1)−C(2)−C(3) 106.8(2), C(2)−C(3)−C(4) 107.4(2), C(3)−C(4)−C(21) 108.7(2), C(4)−C(21)−C(1) 107.2(2), C(6)−N(22)−C(9) 106.3(2), C(11)−N(23)−C(14) 106.6(2), C(16)−N(24)−C(19) 106.2(2), C(21)−Pd−N(22) 90.7(1), N(22)−Pd−N(23) 89.48(9), N(23)−Pd−N(24) 89.55(9), N(24)−Pd−C(21) 90.4(1), C(21)−Pd−N(23) 178.5(1), N(22)−Pd−N(24) 177.17(9).

1.897(3) Å is consistent with the smaller covalent bonding radius of carbon compared to nitrogen. The *trans*-Ni(1)−N(23) bond length of 1.964(2) Å is slightly distended. We have suggested that this 0.03 Å increase in bond length may be the result of a small *trans*-effect caused by the more Lewis basic alkenyl, C(21).[21] Similar 0.05 and 0.04 Å increases in bond length are respectively observed in **18b** and a closely related silver(III) benzocarbaporphyrin.[15a] The *trans*-Ni−N bond length is 0.021(2) Å longer than the *cis*-Ni−N in a related nickel(II) N-confused isoquinoporphyrin;[36] however, all of the Ni−N bond lengths are similar in the case of 2-(2′-bromoethyl)-5,10,15,20-tetraphenyl-2-aza-21-carbaporphyrinato-nickel(II),[37] and 5,10,15,20-tetraphenyl-2-aza-21-carbaporphyrinatosilver(III) shows only a 0.01 Å increase in the *trans*-Ag−N bond length.[4] Although the structural characterizations of two other four-coordinate square planar metal complexes of N-confused porphyrins have been published, these display disorder involving the metal−nitrogen bonds ,and this precludes comparison with our data.[3b,8a] While the small *trans*-effect observed in **14b** and **18b** may indeed be real, the observed metal to ligand bond lengths, as well as the degree of nonplanarity and mode of distortion, are very much influenced by the metric parameters of the ligand framework. Conclusive evidence relating electronic effects to core metric parameters awaits the growth of a database of structurally characterized carbaporphyrins.

When turning to the structure of palladium(II) azuliporphyrin **18b** (Figure 8), it is immediately apparent that the macrocyclic core is significantly more planar than is the case for the nickel(II) complex **14b**. This is evidenced by the pyrrole to mean [18]annulene plane dihedral angles of 9.7(2)°, 4.7(2)°, and 7.4(2)°. However, the azulene to mean [18]-

(36) Xiao, Z.; Patrick, B. O.; Dolphin, D. *Chem. Commun.* **2002**, 1816.
(37) Schmidt, I.; Chmielewski, P. J.; Ciunik, Z. *J. Org. Chem.* **2002**, *67*, 8917.

annulene plane dihedral angle of 15.8(1)° is deceptively large due to the significant 11.6(2)° twist between the azulene's tropylium and cyclopentadienyl rings. The 8.1(2)° cyclopentadienyl to mean [18]annulene plane dihedral angle is more representative of the macrocycle conformation. The palladium(II) ion is situated at the center of the macrocyclic cavity and lies slightly, 0.0148(3) Å, above the C(21), N(22), N(23), N(24) plane. The distances (0.293 Å rms) at which skeletal atoms lie from the plane defined by Pd(1)C(21)N(22)N(23)N(24) classify the porphyrin skeleton as slightly saddled. Particularly illustrative are the β-pyrrolic carbon atom deviations from the plane. These pairs of atoms, C(7)/C(8), C(12)/C(13), and C(17)/C(18), along with the azulene C(3)/C(2) atoms alternate, as pairs, above and below the plane. These atoms also exhibit the seven largest deviations from the plane at −0.458(3), −0.408(3), 0.231(4), 0.239(4), −0.224(3), −0.320(3), and 0.312(3) Å, respectively. The metal is centered between the donor ligands with equivalent *cis*-Pd−N bond lengths of 2.021(2) and 2.016(2) Å. These values fall within the typical 2.012 ± 0.018 Å range reported for palladium-coordinated porphyrin-type macrocycles.[35] The shorter Pd(1)−C(21) bond length of 1.980(3) Å is consistent with the smaller covalent radius of carbon compared to nitrogen. The *trans*-Pd(1)−N(23) bond length is 2.075(2) Å, which, as discussed earlier, represents a 0.05 Å increase in bond length relative to the *trans*-Pd−N parameters. The more planar nature of complex **18b** compared to **14b** illustrates the better size match between the azuliporphyrin cavity and the larger palladium(II) ion relative to the nickel(II) ion. The ions have crystal radii equal to 0.78 and 0.63 Å for the respective square planar coordinated divalent metal ions.[38]

Conclusions

Azuliporphyrins have been shown to readily form organometallic derivatives under mild conditions. Stable complexes have been generated where a central nickel(II), palladium(II), or platinum(II) ion resides within the macrocyclic cavity and binds to all four atoms in the CNNN core. The diamagnetic complexes are easily characterized by spectroscopic and mass spectrometric methods, and two organometallic derivatives were further characterized by X-ray crystallography. These results, together with the easy availability of tetraarylazuliporphyrins via a one-pot Rothemund-type reaction, suggest that azuliporphyrins have the potential to be valuable ligands for the production of unusual coordination complexes and organometallic derivatives.

Experimental Section

Azuliporphyrins **8a**, **8b**, **13a**, and **13b** were prepared as described previously.[23,28,29] NMR spectra were obtained on a Varian Gemini 400 MHz NMR spectrometer and reported in ppm relative to $CDCl_3$ (residual chloroform at 7.26 ppm in proton NMR and $CDCl_3$ triplet at 77.23 ppm in carbon-13 NMR spectra) or d_5-pyridine (residual downfield resonance at 8.71 ppm in proton NMR and the downfield triplet at 149.2 ppm in carbon-13 NMR spectra). These spectra were obtained at 18−21 °C unless otherwise stated. UV−vis spectra were recorded on a Varian Cary UV spectrophotometer. EI mass spectral determinations were made at the Mass Spectral Laboratory, School of Chemical Sciences, University of Illinois at Urbana−Champaign, supported in part by a grant from the National Institute of General Medical Sciences (GM 27029). Elemental analyses were obtained from the School of Chemical Sciences Microanalysis Laboratory at the University of Illinois.

Metal Complexes of *meso*-Unsubstituted Azuliporphyrins. [8,12,13,17-Tetraethyl-7,18-dimethylazuliporphyrinato]nickel(II) (14a). A mixture of azuliporphyrin **8a** (50 mg) and nickel(II) acetate tetrahydrate (50 mg) in DMF (50 mL) was heated for 10 min at 80−90 °C. The mixture was diluted with chloroform and washed with water. The organic solvent was removed in vacuo, and the residue was chromatographed on silica gel eluting with chloroform. Recrystallization from chloroform−hexanes gave the nickel(II) complex **14a** (36 mg, 64%) as brown crystals, mp >300 °C. UV−vis ($CHCl_3$): λ_{max} (log ϵ) 385 (4.74), 454 (4.54), 546 nm (4.36). ^{1}H NMR ($CDCl_3$; 40 °C): δ 1.59 (6H, t, J = 7.6 Hz), 1.64 (6H, t, J = 7.6 Hz), 3.07 (6H, s), 3.42−3.48 (4H, two overlapping quartets), 7.42−7.53 (3H, m), 8.49 (2H, s), 8.93 (2H, d, J = 10 Hz), 9.11 (2H, s). ^{1}H NMR (d_5-pyridine): δ 1.56 (6H, t, J = 7.2 Hz), 1.61 (6H, t, J = 7.6 Hz), 3.07 (6H, s), 3.46 (8H, q, J = 7.6 Hz), 7.47−7.52 (3H, m), 8.89 (2H, s), 9.31 (2H, d, J = 9.6 Hz), 9.64 (2H, s). HRMS (EI): m/z calcd for $C_{36}H_{35}N_3Ni$ 567.2184, found 567.2182.

[8,17-Diethyl-7,18-dimethyl-12,13-diphenylazuliporphyrinato]nickel(II) (14b). A mixture of diphenylazuliporphyrin **8b** (20 mg) and nickel(II) acetate tetrahydrate (25 mg) in DMF (30 mL) was heated for 10 min at 80−90 °C. The mixture was diluted with chloroform and washed with water. The organic solvent was removed in vacuo, and the residue was chromatographed on silica gel eluting with chloroform. Recrystallization from chloroform−hexanes gave the nickel(II) complex **14b** (16 mg, 73%) as iridescent black crystals, mp >300 °C. UV−vis ($CHCl_3$): λ_{max} (log ϵ) 368 (4.82), 466 (4.99), 646 nm (4.40). ^{1}H NMR ($CDCl_3$; 40 °C): δ 1.50 (6H, t, J = 7.4 Hz), 3.06 (6H, s), 3.33 (4H, q, J = 7.4 Hz), 7.36−7.52 (5H, m), 7.54−7.59 (4H, m), 7.75 (4H, d, J = 6.8 Hz), 8.54 (2H, br s), 8.82 (2H, br d), 9.01 (2H, br s). ^{1}H NMR (d_5-pyridine): δ 1.48 (6H, t, J = 7 Hz), 3.09 (6H, s), 3.31 (4H, q, J = 7 Hz), 7.48−7.54 (5H, m), 7.60−7.64 (4H, m), 7.97 (4H, d, J = 7.6 Hz), 9.08 (2H, s), 9.36 (2H, d, J = 8.8 Hz), 9.72 (2H, s). ^{13}C NMR (d_5-pyridine): δ 11.4, 17.0, 19.9, 99.9, 108.5, 128.3, 129.4, 130.1, 132.2, 132.6, 137.0, 138.8, 139.4, 142.6, 143.7, 146.5, 147.8, 151.8, 154.3, 156.0. HRMS (EI): m/z calcd for $C_{44}H_{35}N_3Ni$ 663.2184, found 663.2182. Anal. Calcd for $C_{44}H_{35}N_3Ni$: C, 79.53; H, 5.31; N, 6.32. Found: C, 79.09; H, 5.17; N, 6.41.

[8,12,13,17-Tetraethyl-7,18-dimethylazuliporphyrinato]palladium(II) (15a). A mixture of azuliporphyrin **8a** (26 mg) and palladium(II) acetate (12 mg) in DMF (50 mL) was heated for 10 min at 80−90 °C. The mixture was diluted with chloroform and washed with water. The organic solvent was removed in vacuo, and the residue was chromatographed on silica gel eluting with chloroform. Recrystallization from chloroform−hexanes gave the title palladium(II) complex (28 mg, 93%) as black crystals, mp > 300 °C. UV−vis ($CHCl_3$): λ_{max} (log ϵ) 368 (5.02), 412 (4.98), 447 (4.90), 574 nm (4.28). ^{1}H NMR ($CDCl_3$; 40 °C): δ 1.65 (6H, t, J = 7.6 Hz), 1.68 (6H, t, J = 7.6 Hz), 3.16 (6H, s), 3.46−3.58 (8H, 2 overlapping quartets), 7.44−7.54 (3H, m), 8.57 (2H, br s), 9.03 (2H, br d), 9.18 (2H, br s). ^{1}H NMR (d_5-pyridine): δ 1.62 (6H, t, J = 7.4 Hz), 1.65 (6H, t, J = 7.4 Hz), 3.16 (6H, s), 3.48−3.56 (8H, 2 overlapping quartets), 7.54−7.58 (3H, m), 9.02 (2H, s), 9.43 (2H, m), 9.78 (2H, s). HRMS (EI): m/z calcd for $C_{36}H_{35}N_3Pd$

(38) Shannon, R. D. *Acta Crystallogr., Sect. A* **1976**, *32*, 751.

615.1866, found 615.1863. Anal. Calcd for $C_{36}H_{35}N_3Pd\cdot{}^2/_5CHCl_3$: C, 65.85; H, 5.37; N, 6.33. Found: C, 65.53; H, 5.34; N, 6.22.

[8,17-Diethyl-7,18-dimethyl-12,13-diphenylazuliporphyrinato]-palladium(II) (15b). A mixture of diphenylazuliporphyrin **8b** (25 mg) and palladium(II) acetate (15 mg) in DMF (30 mL) was heated for 10 min at 80−90 °C. The mixture was diluted with chloroform and washed with water. The organic solvent was removed *in vacuo*, and the residue was chromatographed on silica gel eluting with chloroform. Recrystallization from chloroform−hexanes gave the palladium(II) diphenylazuliporphyrin **15b** (21 mg, 72%) as black crystals, mp >300 °C. UV−vis (5% $Et_3N-CHCl_3$): λ_{max} (log ϵ) 380 (4.82), 415 (4.78), 450 (4.69), 580 (4.15), 638 nm (3.92). ^{1}H NMR ($CDCl_3$; 50 °C): δ 1.59 (6H, t, J = 7.6 Hz), 3.14 (6H, s), 3.42 (4H, q, J = 7.6 Hz), 7.33−7.41 (3H, m), 7.51 (2H, t, J = 7.4 Hz), 7.58 (4H, t, J = 7.6 Hz), 7.83 (4H, d, J = 7.2 Hz), 8.75 (2H, br s), 8.81 (2H, d, J = 9.2 Hz), 9.10 (2H, br s). ^{1}H NMR (d_5-pyridine): δ 1.55 (6H, t, J = 7.4 Hz), 3.16 (6H, s), 3.40 (4H, q, J = 7.4 Hz), 7.52 (2H, t, J = 7.6 Hz), 7.57−7.60 (3H, m), 7.63 (4H, t, J = 7.6 Hz), 8.01 (4H, d, J = 7.2 Hz), 9.23 (2H, s), 9.42 (2H, m), 9.82 (2H, s). ^{13}C NMR (d_5-pyridine): δ 11.4, 17.1, 20.0, 100.7, 110.7, 123.4, 126.8, 128.4, 129.4, 132.7, 133.0, 137.7, 137.9, 141.8, 143.3, 149.3, 156.0. HRMS (EI): m/z calcd for $C_{44}H_{35}N_3Pd$ 711.1866, found 711.1882. Anal. Calcd for $C_{44}H_{35}N_3Pd\cdot{}^1/_{10}CHCl_3$: C, 73.15; H, 4.88; N, 5.80. Found: C, 73.28; H, 4.70; N, 5.72.

[8,12,13,17-Tetraethyl-7,18-dimethylazuliporphyrinato]-platinum(II) (16a). A mixture of azuliporphyrin **8a** (26.0 mg) and platinum(II) chloride (16 mg) in DMF (25 mL) was heated under reflux for 15 min. The mixture was diluted with chloroform and washed with water. The organic solvent was removed in vacuo, and the residue was chromatographed on silica gel eluting with chloroform. Recrystallization from chloroform−hexanes gave the title platinum(II) complex (9.5 mg, 27%) as black crystals, mp >300 °C. UV−vis ($CHCl_3$): λ_{max} (log ϵ) 367 (4.97), 427 (4.55), 442 (4.62), 513 (4.34), 551 (4.31), 621 (4.04), 670 (infl, 3.97), 741 nm (infl, 3.56). ^{1}H NMR ($CDCl_3-d_5$-pyridine): δ 1.66 (6H, t, J = Hz), 1.70 (6H, t, J = Hz), 3.19 (6H, s), 3.47−3.55 (8H, 2 overlapping quartets), 7.31 (2H, t, J = 9.6 Hz), 7.63 (1H, t, J = 9.6 Hz), 8.86 (2H, singlet with platinum-195 satellites, $^4J_{Pt,H}$ = 4.4 Hz), 9.24 (2H, d, J = 9.6 Hz), 9.37 (2H, singlet with platinum-195 satellites, $^4J_{Pt,H}$ = 5.3 Hz). HRMS (FAB): m/z calcd for $C_{36}H_{35}N_3Pt$ 704.2479, found 704.2482.

[8,17-Diethyl-7,18-dimethyl-12,13-diphenylazuliporphyrinato]-platinum(II) (16b). A mixture of diphenylazuliporphyrin **8b** (20.0 mg) and platinum(II) chloride (14 mg) in DMF (25 mL) was reacted under the foregoing conditions. Recrystallization from chloroform−hexanes gave the platinum(II) azuliporphyrin **16b** (6.1 mg, 23%) as black crystals, mp > 300 °C. UV−vis (5% $Et_3N-CHCl_3$): λ_{max} (log ϵ) 372 (5.03), 420 (4.62), 442 (4.68), 521 (4.37), 560 (4.41), 629 (4.145), 670 (4.12), 750 nm (infl, 3.63). ^{1}H NMR (d_5-pyridine): δ 1.63 (6H, t, J = 7.4 Hz), 3.23 (6H, s), 3.42 (4H, q, J = 7.4 Hz), 7.35 (2H, t, J = 9.6 Hz), 7.57 (2H, t, J = 7.4 Hz), 7.63−7.70 (5H, m), 7.98 (4H, d, J = 7.2 Hz), 9.09 (2H, singlet with platinum-195 satellites, $^4J_{Pt,H}$ = 4.4 Hz), 9.24 (2H, d, J = 10 Hz), 9.43 (2H, singlet with platinum-195 satellites, $^4J_{Pt,H}$ = 5.6 Hz). ^{13}C NMR ($CDCl_3$-d_5-pyridine): δ 9.1, 14.5, 17.8, 98.6, 110.3, 126.2, 127.1, 130.4, 136.1, 137.4, 138.2, 138.6, 139.6, 157.6. HRMS (EI): m/z calcd for $C_{44}H_{35}N_3Pt$ 799.2458, found 799.2458. Anal. Calcd for $C_{44}H_{35}N_3Pt\cdot{}^1/_3CHCl_3$: C, 58.63; H, 4.78; N, 5.64. Found: C, 58.62; H, 4.87; N, 5.50.

Metal Complexes of *meso*-Tetraaryl Substituted Azuliporphyrins. [5,10,15,20-Tetraphenylazuliporphyrinato]nickel(II) (17a). Tetraphenylazuliporphyrin **13a** (10.0 mg) was heated with nickel(II) acetate tetrahydrate (10 mg) in DMF (10 mL) under reflux for 20 min and the solution cooled to room temperature. The mixture was diluted with chloroform, washed with water, and dried over sodium sulfate. The solvent was evaporated on a rotary evaporator; residual DMF was removed using an oil pump. The residue was chromatographed on a grade III alumina column, eluting with 20% hexanes−dichloromethane. The product was obtained as a green fraction. Recrystallization from chloroform−hexanes gave the nickel(II) complex (8.8 mg; 81%) as lustrous green crystals, mp >300 °C. UV−vis ($CHCl_3$): λ_{max} (log ϵ) 400 (4.84), 468 (4.65), 488 (4.67), 594 (4.15), 649 (4.18), 794 nm (3.54). ^{1}H NMR ($CDCl_3$): δ 6.75 (2H, t, J = 10 Hz), 7.08 (1H, t, J = 9.4 Hz), 7.37 (2H, d, J = 10 Hz), 7.56−7.65 (12H, m), 7.82−7.90 (10H, m), 8.00 (2H, s), 8.06 (2H, d, J = 4.8 Hz). ^{13}C NMR ($CDCl_3$): δ 117.8, 127.2, 127.3, 127.5, 127.9, 129.0, 129.6, 130.0, 132.5, 133.0, 133.5, 133.6, 135.2, 137.7, 141.2, 141.8, 146.5, 148.2, 151.8, 156.5, 166.0. HRMS (FAB): m/z calcd for $C_{50}H_{31}N_3Ni$ + H 732.1950, found 732.1950. Anal. Calcd for $C_{50}H_{31}N_3Ni\cdot{}^1/_2CHCl_3$: C, 76.57; H, 4.01; N, 5.30. Found: C, 76.64; H, 3.85; N, 5.39.

[5,10,15,20-Tetrakis(4-chlorophenyl)azuliporphyrinato]nickel-(II) (17b). Tetrakis(4-chlorophenyl)azuliporphyrin **13b** (10.0 mg) was reacted with nickel(II) acetate tetrahydrate (10 mg) in DMF (20 mL) under the foregoing conditions. Recrystallization from chloroform−hexanes gave the organometallic complex (7.0 mg; 65%) as lustrous green crystals, mp 252−256 °C, dec. UV−vis ($CHCl_3$): λ_{max} (log ϵ) 400 (4.88), 473 (4.69), 490 (4.70), 591 (4.19), 647 (4.21), 796 nm (3.60). ^{1}H NMR ($CDCl_3$): δ 6.91 (2H, t, J = 10.2 Hz), 7.21 (1H, t, J = 9.6 Hz), 7.43 (2H, d, J = 10.4 Hz), 7.56−7.61 (8H, m), 7.76−7.81 (10H, m), 7.97 (2H, s), 8.02 (2H, d, J = 5.2 Hz). ^{13}C NMR ($CDCl_3$): δ 116.8, 127.6, 127.7, 129.7, 130.0, 132.5, 132.9, 134.0, 134.4, 134.5, 134.7, 135.2, 135.8, 138.1, 139.4, 140.0, 146.5, 148.3, 151.7, 156.5, 165.8. HRMS (FAB): m/z calcd for $C_{50}H_{27}Cl_4N_3Ni$ 867.0313, found 867.0314. Anal. Calcd for $C_{50}H_{27}Cl_4N_3Ni\cdot{}^1/_5CHCl_3$: C, 67.43; H, 3.06; N, 4.70. Found: C, 67.60; H, 2.91; N, 4.76.

[5,10,15,20-Tetraphenylazuliporphyrinato]palladium(II) (18a). Tetraphenylazuliporphyrin **13a** (10.0 mg) was heated under reflux with palladium(II) acetate (5 mg) in DMF (10 mL) for 10 min and the solution cooled to room temperature. The mixture was diluted with chloroform, washed with water, and dried over sodium sulfate. The solvent was evaporated on a rotary evaporator; residual DMF was removed using an oil pump. The residue was chromatographed on a grade III alumina column, eluting with 20% hexanes−dichloromethane. The product was obtained as a green fraction. Recrystallization from chloroform−hexanes gave the palladium-(II) complex (7.8 mg; 67%) as a lustrous black powder, mp > 300 °C. UV−vis ($CHCl_3$): λ_{max} (log ϵ) 375 (4.69), 402 (4.83), 481 (4.75), 586 (4.28), 629 (4.26), 791 nm (3.68). ^{1}H NMR (d_5-pyridine): δ 6.96 (2H, t, J = 9.8 Hz), 7.25 (1H, t, J = 10 Hz), 7.61−7.68 (12H, m), 7.71 (2H, d, J = 10.4 Hz), 7.94−7.97 (4H, m), 8.06−8.09 (4H, m), 8.23 (2H, d, J = 5.2 Hz), 8.26 (2H, s), 8.38 (2H, d, J = 4.8 Hz). ^{13}C NMR (d_5-pyridine): δ 119.8, 127.1, 127.3, 127.5, 127.8, 128.2, 129.5, 132.2, 132.5, 132.6, 133.6, 133.9, 136.6, 137.0, 139.3, 142.5, 143.2, 144.9, 147.7, 160.5. HRMS (FAB): m/z calcd for $C_{50}H_{31}N_3Pd$ 779.1553, found 779.1554. Anal. Calcd for $C_{50}H_{31}N_3Pd\cdot{}^1/_8CHCl_3$: C, 75.71; H, 3.94; N, 5.28. Found: C, 75.38; H, 3.74; N, 5.12.

[5,10,15,20-Tetrakis(4-chlorophenyl)azuliporphyrinato]-palladium(II) (18b). Tetrakis(4-chlorophenyl)azuliporphyrin **13b** (10 mg) was reacted with palladium(II) acetate (10.0 mg) in DMF (20 mL) under the foregoing conditions. Recrystallization from chloroform−hexanes gave the organometallic derivative (11.0 mg;

97%) as a black powder, mp > 300 °C. UV−vis ($CHCl_3$): λ_{max} (log ϵ) 374 (4.76), 403 (4.90), 482 (4.82), 587 (4.35), 627 (4.33), 783 nm (3.76). ^{1}H NMR ($CDCl_3$): δ 6.84 (2H, t, J = 10 Hz), 7.16 (1H, t, J = 9.6 Hz), 7.45 (2H, d, J = 10 Hz), 7.57−7.63 (8H, m), 7.75 (4H, AA′XX′ system), 7.86 (4H, AA′XX′ system), 7.92 (2H, d, J = 5.2 Hz), 7.97 (2H, s), 8.04 (2H, d, J = 5.2 Hz). ^{13}C NMR ($CDCl_3$): δ 126.5, 127.4, 127.5, 129.4, 130.2, 132.3 (2), 134.2, 134.5, 134.6, 134.9, 136.1, 136.4, 138.5, 140.6, 141.5, 144.7, 147.7, 149.5, 157.6. HRMS (FAB): *m*/*z* calcd for $C_{50}H_{27}Cl_4N_3Pd$ 914.9994, found 914.9998. Anal. Calcd for $C_{50}H_{27}Cl_4N_3Pd\cdot CHCl_3$: C, 59.05; H, 2.72; N, 4.05. Found: C, 59.38; H, 2.61; N, 4.14.

[5,10,15,20-Tetraphenylazuliporphyrinato]platinum(II) (19a). Tetraphenylazuliporphyrin **13a** (10.0 mg) was heated under reflux with platinum(II) chloride (10 mg) in DMF (10 mL) for 10 min and the solution cooled to room temperature. The mixture was diluted with chloroform, washed with water, and dried over sodium sulfate. The solvent was evaporated on a rotary evaporator; residual DMF was removed using an oil pump. The residue was chromatographed on a grade III alumina column, eluting with 20% hexanes−dichloromethane, and the product was obtained as a green fraction. Recrystallization from chloroform−hexanes gave the platinum(II) complex (3.0 mg; 23%) as a dark green powder, mp >300 °C. UV−vis ($CHCl_3$): λ_{max} (log ϵ) 382 (4.96), 442 (4.71), 466 (4.73), 570 (4.35), 616 (4.24), 774 nm (3.53). ^{1}H NMR ($CDCl_3$): δ 6.66 (2H, t, J = 10 Hz), 7.26 (1H, t, overlaps with residual chloroform signal), 7.56−7.65 (14H, m), 7.87−7.94 (10H, m), 7.97−8.02 (4H, m). ^{13}C NMR (d_5-pyridine; 55 °C): δ 119.3, 124.3, 127.1, 127.3, 127.6, 127.9, 132.2, 133.0, 133.2, 133.3, 133.6, 133.7, 134.1, 135.3, 138.5, 142.1, 142.4, 143.0, 146.5, 149.3, 161.4. HRMS (FAB): *m*/*z* calcd for $C_{50}H_{31}N_3Pt$ 868.2166, found 868.2166.

[5,10,15,20-Tetrakis(4-chlorophenyl)azuliporphyrinato]-platinum(II) (19b). Tetrakis(4-chlorophenyl)azuliporphyrin **13b** (10 mg) was reacted with platinum(II) chloride (10 mg) in DMF (20 mL) under the foregoing conditions. Recrystallization from chloroform−hexanes gave the platinum(II) derivative **19b** (2.75 mg; 22%) as a dark green powder, mp >300 °C. UV−vis ($CHCl_3$): λ_{max} (log ϵ) 383 (4.99), 444 (4.73), 466 (4.75), 567 (4.38), 619 (4.24), 654 (infl, 4.12), 771 nm (3.57). ^{1}H NMR ($CDCl_3$): δ 6.62 (2H, t, J = 10 Hz), 7.24 (1H, t, J = 10 Hz), 7.43 (2H, d, J = 10.8 Hz), 7.56 (4H, AA′XX′ system), 7.61 (4H, AA′XX′ system), 7.71 (4H, AA′XX′ system), 7.84 (4H, AA′XX′ system), 7.91 (2H, doublet, J = 5.2 Hz), 8.04 (2H, d, J = 5.6 Hz, with Pt-195 satellites), 7.99 (2H, singlet with Pt-195 satellites, $^4J_{Pt,H}$ = 5.6 Hz). HRMS (FAB): *m*/*z* calcd for $C_{50}H_{27}Cl_4N_3Pt$ 1004.0607, found 1004.0608.

Cyclic Voltammetry. The electrochemical studies were carried out in anhydrous dichloromethane using a BAS CV-27 potentiostat equipped with an x−y recorder. A conventional three-electrode cell consisting of a platinum disk working electrode, a platinum wire auxiliary electrode, and a $Ag/AgNO_3$ (0.01 M) reference electrode was used. The cyclic voltammograms were run in a 0.2 M Bu_4NBF_4 solution in an inert atmosphere glovebox at a scan rate of 200 mV/s. The scanning limits were +1.7 V to −1.9 V vs $Ag/AgNO_3$, and the ferrocene/ferrocenium couple appeared at +0.22 V vs the $Ag/AgNO_3$ reference. All potentials are reported vs the $Ag/AgNO_3$ reference electrode.

Crystal Structure Determination of 14b and 18b. Crystal data and a summary of the intensity data and collection parameters for **14b** and **18b** are given in Table 1. X-ray data for the two compounds were collected using a Bruker P4/R4/SMART 1000 CCD diffractometer equipped for Mo Kα radiation (λ = 0.71073 Å), at −80 °C. Data collection and cell refinement were performed using SMART.[39a] Data reduction was accomplished using SAINT.[39b] Empirical absorption correction was performed on the data from **14b** through the use of the SADABS procedure.[39c] Face-indexed absorption correction by integration was performed on the data from the triclinic crystal of **18b** using SHELXTL.[39d] Solution and data analysis were performed using the WinGX software package.[40] Both structures were solved using the direct methods program SIR-92.[41] The remaining atoms were located using difference Fourier synthesis, and full-matrix least-squares refinement on F^2 that led to a convergence was performed using SHELXL-97.[42] With the exception of a solvent molecule in **18b**, non-hydrogen atoms were refined with anisotropic thermal parameters. Hydrogen atoms were assigned positions based on the geometries of their attached carbon atoms, and were given isotropic thermal parameters 20% greater than their parent carbon atoms.

X-ray quality crystals of **14b** were obtained by diffusion of hexanes into dichloromethane. A dark green rod thereby obtained of approximate dimensions 0.60 × 0.05 × 0.05 mm^3 was mounted on a glass fiber with super-glue and transferred to the diffractometer. Limiting indices were as follows: $-38 \le h \le 38$, $-11 \le k \le 10$, $-13 \le l \le 14$. The structure was refined to convergence, $(\Delta/\sigma)_{max}$ = 0.006; a final difference Fourier synthesis showed features in the range $\Delta\rho_{max}$ = 0.746 e Å^{-3} to $\Delta\rho_{min}$ = −0.502 e Å^{-3} and were deemed of no chemical significance. This structure was previously communicated,[21] but the detailed analysis is provided in this Article.

X-ray quality crystals of **18b** were obtained by slow evaporation of chloroform. A pale brown plate thereby obtained of approximate dimensions 0.50 × 0.24 × 0.06 mm^3 was mounted on a glass fiber with super-glue and transferred to the diffractometer. Limiting indices were as follows: $-15 \le h \le 15$, $-16 \le k \le 14$, $-18 \le l \le 18$. In addition to the parent molecule, 1.1667 $CHCl_3$ molecules were located in the asymmetric unit. The first solvent molecule was readily observed in the initial SIR-92 solution and was refined anisotropically. The remaining partial occupancy, disordered solvent was located from difference Fourier synthesis and is poorly behaved. The best model gave $^1/_3$ of a chloroform solvent molecule located with the carbon atom 0.58 Å from, and disordered about, a crystallographic inversion center; thus, atoms of this $CHCl_3$ were treated as having $^1/_6$ occupancy in the asymmetric unit. To establish reasonable bonding parameters, this $CHCl_3$ molecule was constrained such that all C−Cl distances were isometric, and all Cl−Cl separations were isometric. Isotropic refinement gave 1.80(3) Å C−Cl and 1.07(2)° Cl−C−Cl bond angles for the disordered $CHCl_3$ molecule. The structure was refined to convergence, $(\Delta/\sigma)_{max}$ = 0.001; a final difference Fourier synthesis showed features in the range $\Delta\rho_{max}$ = 0.98 e Å^{-3} to $\Delta\rho_{min}$ = −0.616 e Å^{-3}. These peaks are in the vicinity of the full occupancy chloroform solvent. The 10 largest residual electron density peaks all lie within 1 Å of a chlorine or the palladium atom, and were deemed to be of minimal structural and of no chemical significance.

Complete X-ray structural data has been deposited at the Cambridge Crystallographic Data Center, CCDC No. 179074 and

(39) (a) Bruker *SMART 1000 CCD software package*; Bruker Advanced X-ray Solutions: Madison, WI, 1999. (b) Bruker *SAINT Integration Software for Single-Crystal Data frames—h, k, l, intensity*; Bruker Advanced X-ray Solutions: Madison, WI, 1999. (c) Bruker *SADABS—Empirical adsorption correction procedures*; Bruker Advanced X-ray Solutions: Madison, WI, 1999. (d) SHELXTL—*Program for crystal structure analysis*; Bruker Advanced X-ray Solutions: Madison, WI, 1997.

(40) (a) Farrugia, L. J. *J. Appl. Crystallogr.* **1999**, *32*, 837. (b) Farrugia, L. J. *J. Appl. Crystallogr.* **1997**, *30*, 565.

(41) Altomare, A.; Cascarano, G.; Giacovazzo, C.; Guagliardi, A. *J. Appl. Crystallogr.* **1993**, *26*, 343.

(42) Sheldrick, G. M. *SHELXS-97*; 97-2 ed.; Programs for X-ray Structure Determination; University of Göttingen: Göttingen, Germany, 1997.

No. 211045. Copies of this information may be obtained free of charge from The Director, CCDC, 12 Union Road, Cambridge CB2 1EZ, U.K. (Fax, + 44-1223-336033; e-mail, deposit@ccdc.cam.ac.uk; URL, http://www.ccdc.cam.ac.uk).

Acknowledgment. This material is based upon work supported by the National Science Foundation under Grants CHE-9732054 and CHE-0134472 (to T.D.L.) and the donors of the Petroleum Research Fund, administered by the American Chemical Society (to T.D.L. and G.M.F.). D.A.C. received additional funding from the Barry M. Goldwater Foundation, the Johnson and Johnson Travel Award Program, and Pfizer Inc. We also thank Dr. Robert McDonald and The University of Alberta Structure Determination Laboratory for the collection of low-temperature CCD X-ray data.

Supporting Information Available: UV−vis, ^{1}H NMR, ^{13}C NMR and mass spectra for selected compounds. Tables of crystallographic details, atomic coordinates, bond lengths and angles, critical angle planes, torsional angles, anisotropic thermal parameters, and hydrogen atom parameters for azuliporphyrin derivatives **14b** and **18b**. Crystallographic data in CIF format. This material is available free of charge via the Internet at http://pubs.acs.org.

IC030166B